

## **DETERMINATION OF PARAMETERS GENERATING THE REFERENCE PRESSURE IN THE PRIMARY LEVEL DYNAMIC PRESSURE MEASUREMENT SYSTEM BASED ON THE DROP WEIGHT METHOD**

**Recep Yılmaz<sup>1,2)</sup>, Hüseyin Arıkan<sup>2)</sup>, Yasin Durgut<sup>1)</sup>, Abdullah Hamarat<sup>1)</sup>**

1) TÜBİTAK National Metrology Institute, TÜBİTAK Gebze Yerleşkesi P.K.54, 41470 Gebze, Kocaeli, Türkiye  
(✉ [yilmaz.recep@tubitak.gov.tr](mailto:yilmaz.recep@tubitak.gov.tr))

2) Necmettin Erbakan University, Faculty of Engineering, Institute of Natural and Applied Science, Yeni Meram Boulevard Kasım Halife Street 11, 42090 Meram, Konya, Türkiye

### **Abstract**

For some industries such as automotive, defence, aerospace, pharmaceutical manufacturing, dynamic pressure measurement is an important requirement. In a primary level dynamic pressure measurement system with a drop weight method, the dynamic pressure value is calculated using parameters such as the effective area value depending on the piston cylinder unit, the maximum acceleration value measured by a laser interferometer. On the other hand, the type of liquid used in the measuring head is another important factor affecting repeatability and providing ease of measurement. In this study, a new measurement head, piston and cylinders were designed, manufactured and the Taguchi method was used to accurately determine some parameters affecting the measurements in a dynamic primary pressure measurement system operating with the drop weight method. In the studies carried out, four pistons, four cylinders, four sampling frequency values and two liquid types were considered. By using the Taguchi method, the optimum parameters of the dynamic pressure measurement system with drop weight method were determined with only sixteen experiments instead of one hundred and twenty-eight.

**Keywords:** Dynamic pressure, drop weight, Taguchi method, laser interferometer, low pass filter, effective area.

© 2024 Polish Academy of Sciences. All rights reserved

### **1. Introduction**

At the microscopic level it is said that pressure is the result of the transfer and motion of the momentum of a liquid or gas to a surface. On the other hand, at a macroscopic level generally pressure is explained as the total force, perpendicular to a surface area, as given in (1)

$$p = \frac{F}{A}. \quad (1)$$

In (1)  $p$  is the pressure,  $F$  is the force and  $A$  is the area. The pressure value is defined as static when it remains constant for a significant period of time and is generally expected to remain unchanged throughout the entire measurement. However, apart from static pressure, there are also situations where it pressure changes in a short time interval. In this case, the pressure value is no longer static but dynamic. When talking about dynamic pressure, the measured quantity is not a single pressure value that does not change with time, but a time-dependent pressure function as given in (2).

$$p = p(t). \quad (2)$$

Transducers frequently are used in static and dynamic pressure measurements according to the type of the work is done. Some applications have characteristics that do not change over time, namely static, and static types of pressure sensors are used to measure the static pressure in question. However, if the relevant pressure value is not a constant value but changes depending on time, such pressure is defined as dynamic pressure and to measure this type of pressure, dynamic pressure sensors are used. The main difference between a static pressure transducer and a dynamic pressure transducer lies in their ability to measure pressure in different fluid conditions. Static pressure transducers are suitable for measuring steady and stable pressure in static or constant flow conditions while dynamic pressure transducers are used to measure pressure fluctuations and rapid pressure changes in the fluid flow.

Dynamic pressure sensors are used in applications in many fields at amplitudes from a few pascals to several giga pascals and in these applications, dynamic pressure measurements that vary depending on time are needed [1, 2]. As with all measuring instruments, pressure sensors need to be calibrated. During dynamic calibration, the pressure value changes significantly in a short time interval like three or six milliseconds and its shape is generally a half sinus signal similar to a parabola [3]. Dynamic pressure transducers with very fast response times are used to measure dynamic pressure reliably. Calibration of this type of transducer against a reference dynamic pressure to be applied is still required. Many applications of the mechanical quantities of force, torque and pressure measurements are of the dynamic type, that is, the measurand varies strongly with time. However, the calibration of the respective transducers is currently being performed mostly according to static procedures. One reason for this is lack of internationally accepted standards and methods in the field of dynamic calibrations [4]. Dynamic calibration of a pressure sensor, or dynamic pressure measurement, involves revealing and analysing the dynamic behaviour of the calibrated sensor in accordance with the measurement accuracy needed at the place where the sensor will be used. In dynamic pressure calibration, reliable, controllable and well-known dynamic pressure whose value changes over time must be produced to be applied to the sensor to be calibrated with the reference dynamic pressure standard. The generated dynamic pressure value is applied to the sensor to be used as the reference pressure value for the dynamic pressure sensor to be calibrated, also called the test sensor, and the pressure or electrical load response produced by the sensor is measured.

There are several methods of obtaining a pressure pulse in a dynamic pressure measurement system such as the shock tube [5], a step pressure generator using a fast-opening valve [6], or the drop weight. In this last method, a mass is dropped from a certain height onto a piston-cylinder unit attached to a measuring head containing pressure-transmitting liquid. At the same time, a dynamic pressure transducer to be calibrated is connected to the measuring head [7]. In the drop-weight method, before the mass hits the piston-cylinder unit, the dynamic pressure transducer senses a small static pressure created by the piston weight and the hydrostatic pressure of the pressure-transmitting liquid. When peak pressure is reached, pressure is created by the weight of the piston and the drop weight with hydrostatic pressure created by the pressure-transmitting liquid. In

the drop-weight method, the obtained pressure consists of dynamic and static characteristics called the total pressure. While the piston weight and the hydrostatic pressure of the pressure-transmitting liquid generate static pressure, as of the dropping mass hits the piston, the dynamic component of the total pressure is generated. In practice, the effect of the piston weight and the hydrostatic pressure of the pressure-transmitting liquid account for less than 0.01% of even the smallest pressure pulses [8]. Therefore, these effects are neglected. In a primary level system, the reference pressure must be calculated by the operator using the piston cylinder unit effective area value, the acceleration value measured by the laser interferometer, the drop weight value and the local gravity acceleration parameters. From the calculation parameters, the effective area value depending on the piston-cylinder unit and the maximum acceleration change measured at the point where the drop weight hits the piston should be well known to calculate a more precise dynamic pressure value. It is difficult to obtain the correct data at the point where the acceleration is maximum, especially due to the high noise occurring in the acceleration signals received by the laser interferometer. However, a good approximation can be obtained when a low-pass filter with a well-chosen cut-off frequency value is applied to the acceleration signal. But even in this case, some frequencies may overlap [8]. As a part of this study, a low-pass filter selection and application have been performed on the acceleration signals obtained from the laser interferometer and used in the reference dynamic pressure calculation.

In addition to these parameters, the compatibility of the liquid used in the measuring head, the piston and the cylinder unit is another important factor to be examined. In a study on the change in the refractive index of a compressed fluid, the difference between adiabatic and isothermal compression of fluids was investigated. The liquids studied were sebacate, glycerol and water. In the study, sebacate was evaluated as the most suitable measuring fluid for dynamic pressure measurements using low weight masses [9]. However, in different studies, glycerol was preferred as the liquid used in the measuring head [8, 10]. In order to investigate the effect of this parameter on repeatable measurements, both fluids used in the measurements have to be evaluated in experiments.

Besides the liquid used in the measurements, there are four pistons and four cylinders with a nominal diameter of ten mm that we have designed and produced to use in our dynamic pressure measurement system and to observe its effect. It was done deliberately as the nominally determined mass release height from the electromagnet aimed to achieve a certain pressure may change after each drop due to fluid leakage under pressure from the gap between the piston and the cylinder. This is not desirable in terms of ease of measurement and repeatability.

Another factor that can affect the measurement results is the sampling frequency used when collecting data from the laser interferometer. Normally, higher sampling frequency selections are expected to produce better results, but higher sampling frequencies require faster converters and more storage space. Therefore, researchers must evaluate the advantages and disadvantages of each application. When the sampling frequency is set too high, the noise ratio increases, and if it is set too low, there is a risk of not catching the real peak value of the signal. In this respect, the four sampling frequency values were determined as 10 kHz, 25 kHz, 50 kHz and 100 kHz.

In order to examine the effects of all determined parameters on the measurement results, a total of 128 different experiments is required. Considering that five repetitions will be made in each experiment, the total number of measurements will be 640. When this is evaluated in terms of time and cost, it seems quite troublesome. In this context, the Taguchi method was used in the experiments. The Taguchi method is very useful for determining the best combination among different levels of different parameters. In cases where a lot of experimental work needs to be done for all combinations containing each level of each parameter, it is possible to reach the result with a much smaller number of experimental studies by using the orthogonal array table in the

Taguchi method [11, 12]. In the determination of the parameters mentioned above, by using the Taguchi method, the optimum parameters can be selected with only 16 experiments instead of 128 experiments, when we evaluate it as the number of measurements, it is only 80 measurements instead of 640 measurements.

## 2. Primary dynamic pressure measurement standard

In a primary designed dynamic pressure measurement system, there are various components such as servo motors, a laser interferometric system, an electromagnet, guiding rods, a drop weight, a rebound system, a measuring head, a piston and cylinder unit and *etc.* A schematic view of a primary level dynamic pressure measurement system and its components developed with the drop weight method is given in Fig. 1.

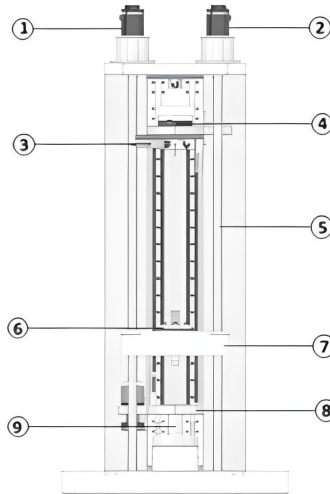


Fig. 1. A schematic view of a primary level dynamic pressure measurement system developed with the drop weight method. (1 and 2 - servo motors, 3 – laser interferometer, 4 – electromagnet, 5 – guiding rod, 6 – laser retroreflector, 7 – drop weight, 8 – rebound system, 9 – measurement head, piston and cylinder).

With one of the servo motors used in the system, the mass is lifted to a certain height by the electromagnet and left for a free fall on the piston. The reference standard device runs with the principle of free-falling mass, according to the physical law of conservation of energy. The drop weight system transfers the movement energy gained by the free-falling mass during the free fall by falling on a piston, and the piston is shifted to the test sensors connected to the same chamber with this instantaneous force transferred by the fluid filling this chamber, and thus the energy of the falling mass reaches the test sensors to be calibrated. The created reference dynamic pressure is calculated with the formula given in (3) [8].

$$p = \frac{m_{\text{total}}(g + a)}{A_{\text{eff}}}, \quad (3)$$

where  $p$  is the dynamic pressure value to be calculated,  $m_{\text{total}}$  is the total mass value of the drop weight with the laser retroreflector, the oil in the measuring head and the piston,  $g$  is the local gravity value,  $a$  is the maximum acceleration change in the signal obtained from the laser interferometer

when the drop weight first hits the piston and  $A_{\text{eff}}$  is the effective area value calculated using data from dimensional measurements of the piston and cylinder unit. Here, it is necessary to calculate the effective area value ( $A_{\text{eff}}$ ) and acceleration value ( $a$ ) by utilizing some applications. The effective area calculations are performed with the dimensional measurement method depending on the pistons and cylinders. The acceleration values are calculated by processing the data obtained from the laser interferometer.

In the schematic image of the drop-weight system shown in Fig. 1, some important components used in the measurement system are indicated with sequence numbers. More detailed pictures of these components are given in Fig. 2, again according to their numbers in Fig. 1.

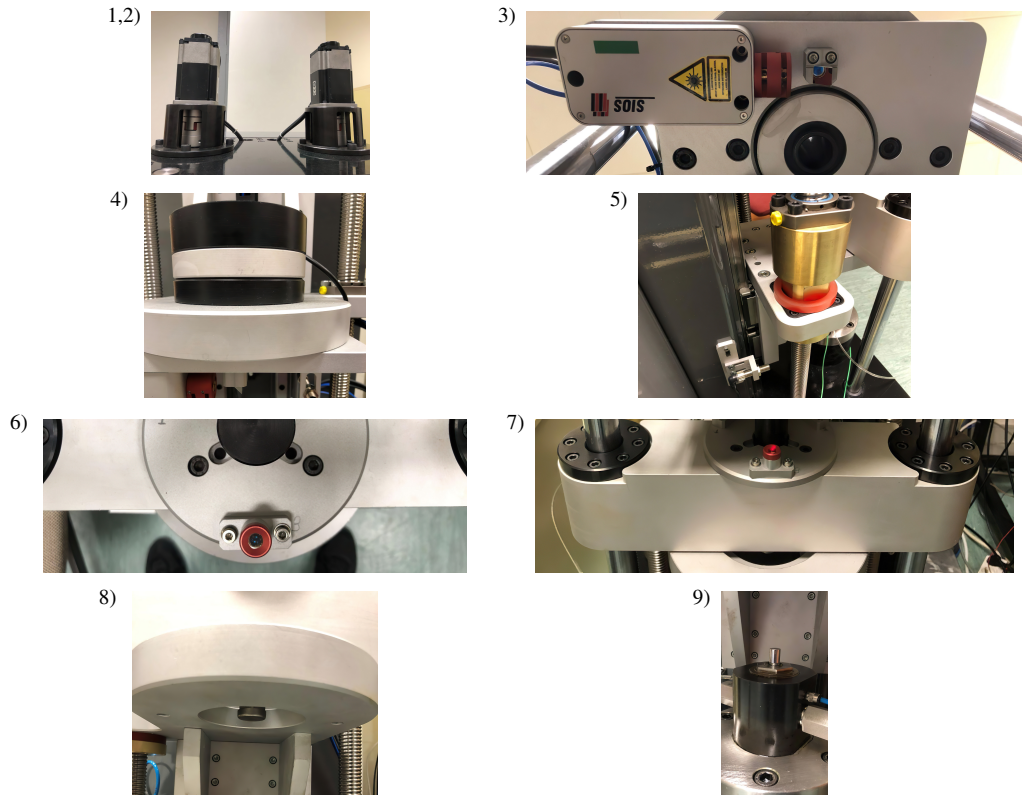


Fig. 2. Selected components of a primary level dynamic pressure measurement system developed by the drop weight method. (1 and 2 - servo motors, 3 – laser interferometer, 4 – electromagnet, 5 – guiding rod, 6 – laser retroreflector, 7 – drop weight, 8 – rebound system, 9 – measurement head, piston and cylinder).

Four pistons, four cylinders and a measuring head, which contains the pressure transmission fluid, that are connected to the piston cylinder unit and sensors have been designed and produced to be used in the primary level dynamic pressure measurement system. The reason why pistons and cylinders are produced in four pieces is to determine the most suitable combination that can provide repeatable measurements. In this way, it is aimed to reduce the amount of liquid leaking from the gap between the piston and the cylinder during the measurement. The design and production of the measuring head, piston cylinder and assembly drawing are given in Fig. 3. Also, the working principle of the dynamic pressure measurement system with the drop-weight method is given in Fig. 4.

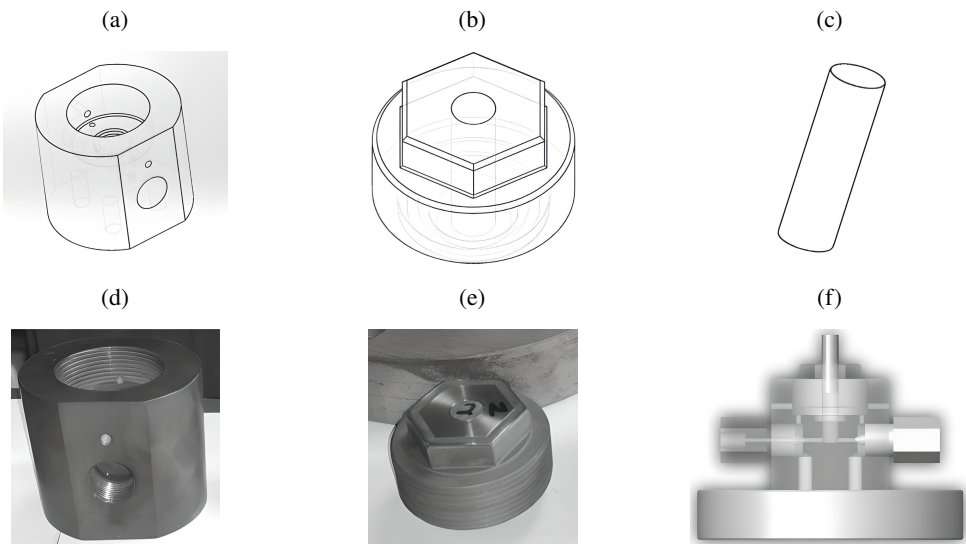


Fig. 3. 3D model of the measuring head (a), 3D model of the cylinder (b), 3D model of the piston (c), finished measuring head (d), finished piston-cylinder unit (e) and transparent assembly image (f).

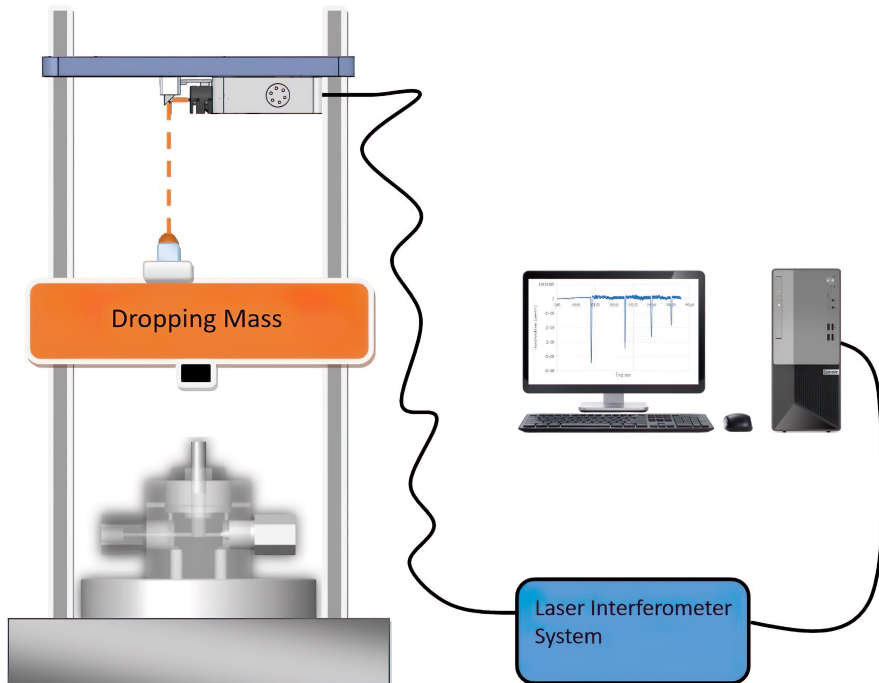


Fig. 4. The working principle of the dynamic pressure measurement system with the drop-weight method.

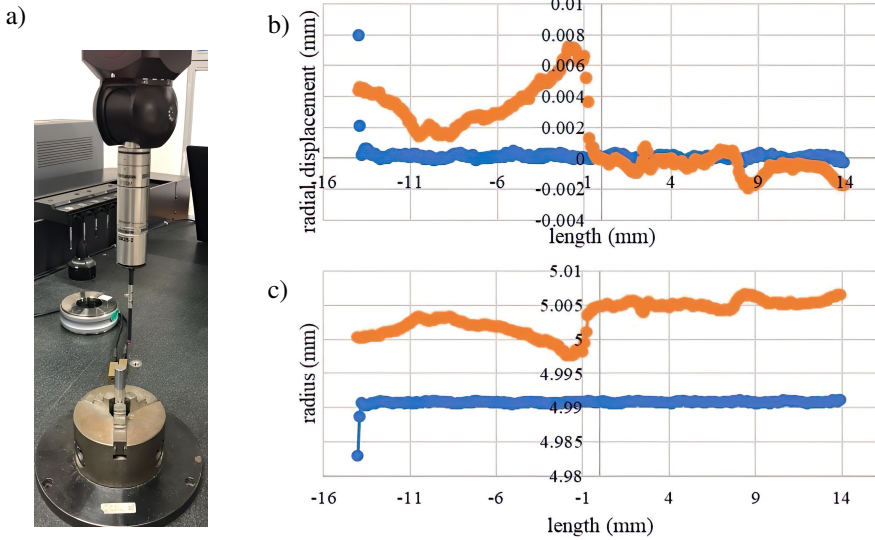


Fig. 5. A section from the measurement made with the CMM device (a), radial displacements (b) and radius values (c) of the number one piston and number one cylinder unit.

In the Fig. 4 the dropping mass is dropped onto the piston from a certain height, while data is collected with the laser interferometer system. At the very moment when the mass hits the piston, the amplitude of the acceleration reaches its absolute maximum value. On the other hand, in order to calculate the reference pressure according to (3), it is necessary to calculate the effective area of the piston and cylinder unit on which the mass drops.

### 3. Calculations of the effective area of the piston-cylinder units

The data to be used in the effective area calculation were obtained with the dimensional measurement method using the *coordinate measuring machine* (CMM). In the measurements made with the CMM, the measurements were taken on the 28 mm parts of the 35 mm long pistons and cylinders. The reason for this is that only these parts work together. For pistons and cylinders, measurements were taken at 8 points at 45-degree intervals for each diameter [13]. After the measurement was completed at 8 points of each diameter, the CMM device moved in the z direction of 0.1 mm and the measurements continued in this way for the 28 mm distance. There were 2240 measuring points in total, including x, y and z coordinates for each part. Figure 5 shows a section from the measurement of the piston made with the CMM device and the graphs showing the radial displacement and radius values along the z-axis calculated using the CMM data of the number one piston and the number one cylinder.

There are several different ways to calculate the effective area value using dimensional measurement data [14]. One of them, Dadson's theory, is given in (4) [15].

$$A_0 = \pi r_0^2 \left[ 1 + \frac{h_0}{r_0} + \frac{1}{r_0 l} \int_0^l (u(x) + U(x)) dx \right], \quad (4)$$

where  $A_0$  is the effective area value of the piston-cylinder unit at zero pressure,  $r_0$  is the radius value of the piston and  $h_0$  is the radial gap between the piston and cylinder at the point of  $z = 0$ ,  $l$

is the engagement length of the piston and cylinder, and  $u_x$  and  $U_x$  values represent the radial displacements of the piston and cylinder along the  $z$ -axis, respectively.

Three different methods are used to calculate the numerical integral value in Dadson's theory. One of them is Simpson's 3/8 rule [14]. In (4), when we determine the values of  $r_0$  and  $h_0$  for  $z = l/2$ , that is, for the middle of the piston and the cylinder along the same working length, the integral value in the formula will not change. In this case, the formula will be used as given in (5).

$$I = \int_{-l/2}^{l/2} (u(x) + U(x))dx = I_1 + I_2 \tag{5}$$

The value of  $I$  given in (5) is divided into  $I_1$  and  $I_2$  and is shown in (6) and (7), respectively.

$$I_1 = \int_{-l/2}^{l/2} (u(x))dx \tag{6}$$

$$I_2 = \int_{-l/2}^{l/2} (U(x))dx \tag{7}$$

According to Simpson's 3/8 rule, we can calculate  $I_1$  and  $I_2$  values according to the equations given in (8) and (9), respectively.

$$I_1 = w \sum_{i=0}^n \frac{u(x_i) + 3u(x_{i+1}) + 3u(x_{i+2}) + u(x_{i+3})}{8} \tag{8}$$

$$I_2 = w \sum_{i=0}^n \frac{U(x_i) + 3U(x_{i+1}) + 3U(x_{i+2}) + U(x_{i+3})}{8} \tag{9}$$

The effective area values of the piston and cylinder units obtained from the calculations using (4), (8) and (9) are given in Table 1.

Table 1. Effective area results of the piston and cylinder units in mm<sup>2</sup>.

|           | s1          | s2          | s3          | s4          |
|-----------|-------------|-------------|-------------|-------------|
| <b>p1</b> | 78.49718794 | 78.46020172 | 78.39135945 | 78.44079162 |
| <b>p2</b> | 78.50562772 | 78.39978672 | 78.39978672 | 78.44922473 |
| <b>p3</b> | 78.51914016 | 78.48214770 | 78.41329382 | 78.46273432 |
| <b>p4</b> | 78.50270377 | 78.39686978 | 78.39686978 | 78.44630452 |

The effective area values in Table 1 will be used to calculate the results of the measurements in the Taguchi experimental design. Also, the uncertainty of the effective area of the piston-cylinder unit is derived from dimensional measurements and, according to Dadson's theory, can be expressed in (10) [15].

$$\frac{u(A_0)}{A_0} = \frac{2u(r)}{(A_0/\pi)^{0.5}}, \tag{10}$$

where  $u(r)$  is the uncertainty value from dimensional measurements,  $A_0$  is the effective area value of the piston and cylinder unit.



#### 4. Determination of acceleration values obtained with the laser interferometer

In order to accurately calculate the reference dynamic pressure with the primary level dynamic pressure measurement system, it is necessary to correctly determine the maximum acceleration value at the point where the signal peaks, which is another important parameter, after the effective area values. In the studies carried out in the laboratory, it has been determined that the most important parameter affecting the reference dynamic pressure calculation is the acceleration ( $a$ ) value. For instance, a  $10 \text{ m/s}^2$  change in acceleration at 50 MPa pressure value causes an error of approximately 2%. Therefore, the acceleration signals obtained from the laser interferometer will be examined in detail and optimum acceleration values will be obtained. Within the scope of this study, all measurements were carried out by dropping the mass onto the piston from a distance of 16 mm. This distance is set by taking the highest point of the piston as reference. Figure 6 shows an example of a signal obtained from the laser interferometer showing the acceleration values against time without low pass filtering while the mass was dropped from the 16 mm height and hit the piston.

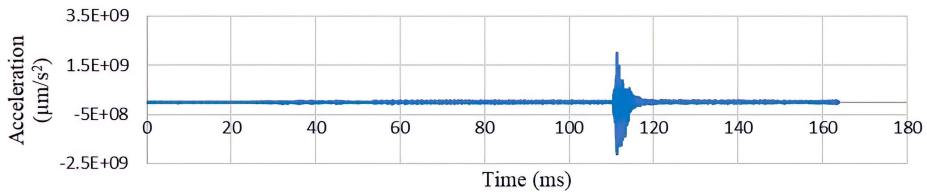


Fig. 6. An example signal obtained from laser interferometer without a low pass filter.

If we get closer to the signal in Fig. 6 from the peak point, the new signal will be like in Fig. 7.

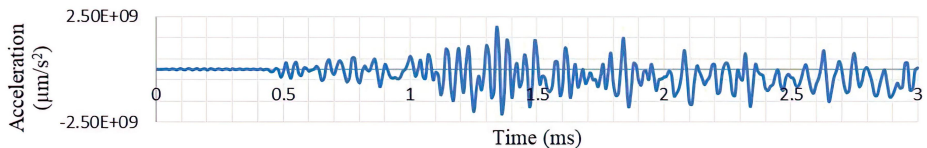


Fig. 7. A zoomed-in view of a sample signal obtained from a laser interferometer without a low-pass filter at the peak.

In electronics, there are always some unwanted components in the transmitted signal. Such unintentionally transmitted signals are called interference, parasitic signals or noise. As it is clearly seen in Fig. 6 and Fig. 7, the absolute maximum acceleration value is so high that it is not possible to calculate the peak value we are looking for from such a signal due to the noise on the signal. Thus, the signal is filtered with a suitable low pass filter, but here we have another problem, determining an appropriate cut-off frequency. Low pass filters pass all values below the frequency determined in the signal to which it is applied and weaken the values above it. Therefore, the most appropriate cut-off frequency should be determined in order not to lose the important acceleration value in the signal. The work done to determine the cut-off frequency is shown in Fig. 8.

In Fig. 8, low-pass filters with different cut-off frequencies were applied to the acceleration signals obtained by the laser interferometer and the acceleration values at the maximum point were examined. Figure 9 shows acceleration values against low-pass filters in the (0-2) kHz range obtained from the graphic values given in Fig. 8.

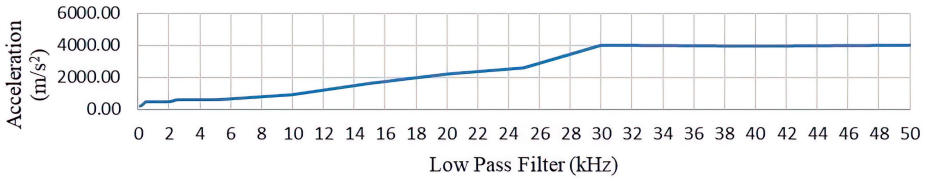


Fig. 8. Cut-off frequency determination study for low pass filter.

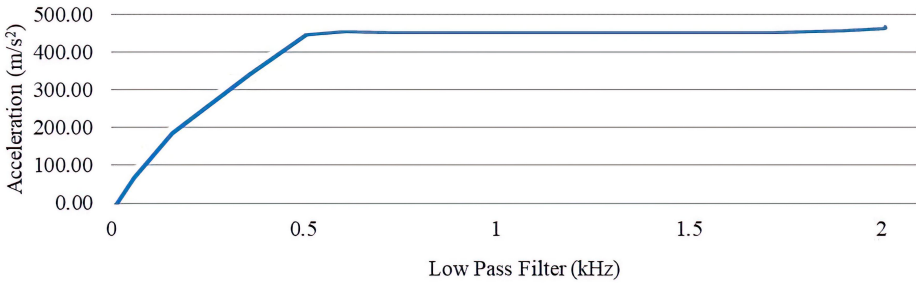


Fig. 9. Determining the cut-off frequency for a low-pass filter in the (0-2) kHz range.

Based on the data obtained from the graph in Fig. 9, the cut-off frequency to be used in the acceleration detection studies was determined as 1500 Hz. The range that is important to us is one that does not change much as the low-pass filter value changes [16]. However, another important issue here is that when choosing a low-pass filter at a low frequency value, the signal to noise ratio decreases, and the risk of losing the actual acceleration data at the peak point increases. For this reason, it should not be forgotten that the situation may change for different signals and sampling frequencies, even if there is not much change in the data for low-pass filter values with a low frequency value. Above the 1500 Hz low-pass filter value, for example at 2000 Hz, the change in the acceleration data has not yet started, but as can be seen in Fig. 9, this point is almost the limit where the change starts. In addition, as the low-pass filter frequency value increases, as in Fig. 8, there is a significant noise factor in the data and it becomes impossible to get correct data from the signal. The graph showing the peak form and values of the filtered signal with different low-pass filter frequency values is given in Fig. 10.

As can be seen in Fig. 10, the signal starts to deteriorate gradually at the cut-off frequency values after 1500 Hz. Therefore, the cut-off frequency of 1500 Hz is suitable for our work. The new signal obtained when a 1500 Hz low-pass filter is applied to a different signal is shown in Fig. 11.

If we enlarge the largest peak in Fig. 11, we can see the peak point of the signal closer and examine its form. Figure 12 shows the zoomed-in part of the peak point.

The measurements made with the laser interferometer were evaluated in this way and the acceleration values to be used in the measurement calculations specified in the Taguchi experimental design are given in Table 2.

Table 2 contains some empty cells because it was noticed that acceleration data for these measurements could not be obtained after the measurements were completed. However, since the averages of repeated measurements will be used when calculating the reference pressure values, the results will not be affected by this situation. While determining the values in Table 2, the peak-to-peak situation where the maximum change in acceleration occurred was taken into account and the data obtained were evaluated as absolute. The uncertainty value coming from the laser interferometer used to calculate the maximum acceleration value can be considered as the most

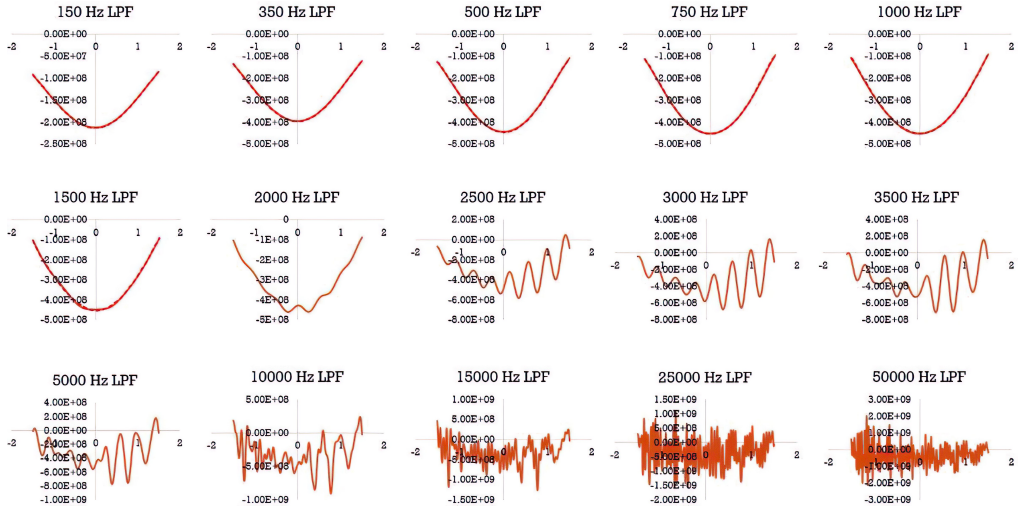


Fig. 10. Peak form and values of the filtered signal with different low-pass filter frequency values.

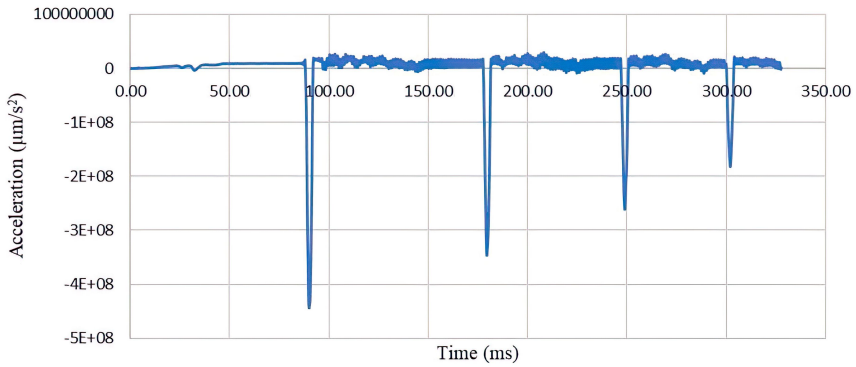


Fig. 11. A low-pass filtered acceleration signal of 1500 Hz.

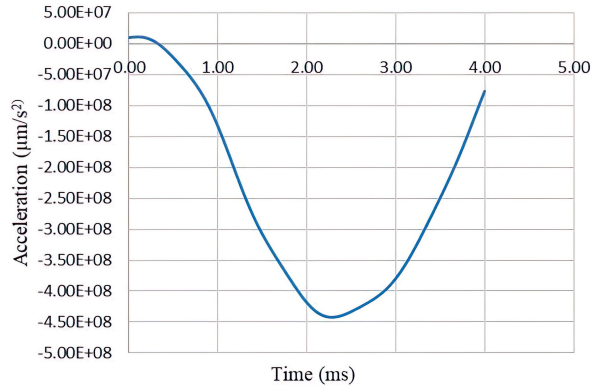


Fig. 12. Zoomed-in part of the peak point of the largest peak in Fig. 11.

Table 2. The acceleration values obtained from the laser interferometer to be used in the measurement calculations.

| 1                | 2                | 3                | 4                | 5                | Average          |
|------------------|------------------|------------------|------------------|------------------|------------------|
| m/s <sup>2</sup> | m/s <sup>2</sup> | m/s <sup>2</sup> | m/s <sup>2</sup> | m/s <sup>2</sup> | m/s <sup>2</sup> |
| 464.32           | 461.79           | 461.65           | 463.55           | 465.63           | 463.39           |
| 467.81           | 457.52           | 459.06           | 458.29           | 460.61           | 460.66           |
| 464.52           | 461.96           | 464.36           | 470.06           | 470.10           | 466.20           |
| 469.93           | 467.53           | 469.94           | 475.44           | 479.87           | 472.54           |
| 463.35           | 458.12           | 455.95           | 456.51           | 457.79           | 458.34           |
| 478.97           | 468.53           | 464.68           | 461.89           | 465.84           | 467.98           |
| 475.31           | 465.06           | 474.71           | 478.07           | 481.97           | 475.03           |
| 453.16           | 453.37           | 459.61           | 469.14           | 474.56           | 461.97           |
| 325.80           | 326.87           | 328.05           | 330.96           | 332.62           | 328.86           |
| 330.72           | 332.70           | 335.07           | 337.48           |                  | 333.99           |
| 330.79           | 325.41           |                  | 325.62           | 324.87           | 326.67           |
| 339.17           | 332.99           | 333.63           | 335.78           | 335.74           | 335.46           |
| 349.60           | 361.29           | 372.56           |                  |                  | 361.15           |
| 364.04           | 368.79           | 392.45           |                  |                  | 375.09           |
| 343.88           | 356.36           | 364.31           | 370.41           | 379.63           | 362.92           |
| 336.23           | 339.66           | 345.80           | 352.51           | 360.24           | 346.89           |

critical uncertainty value for the measurement. This uncertainty is mostly due to noise in the signal and other uncertainties of the laser interferometer. As shown in Fig. 9 s, the place where the acceleration change in the between 1 kHz and 1.5 kHz range is at its maximum can be considered as the acceleration uncertainty caused by noise. [8].

### 5. Taguchi method for the parameters to be determined

The piston, cylinder and fluid to be used in the produced measuring head should be decided. In this context, we have four pistons (p1, p2, p3, p4), four separate cylinders (s1, s2, s3, s4) and two separate media fluids (glycerol and sebacate) that we can use. The media fluids are given in Fig. 13 and their properties are given in Table 3.

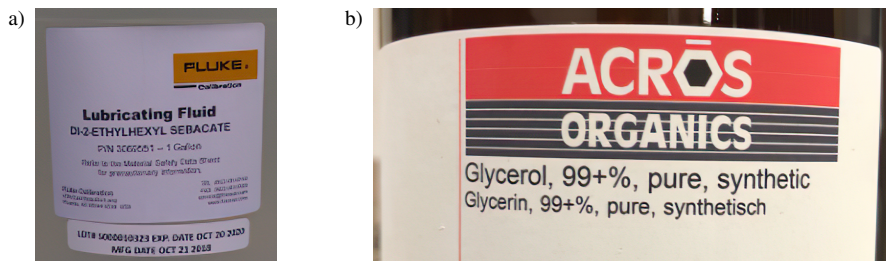


Fig. 13. Sebacate (a), glycerol (b).

Table 3. Media fluids properties.

| Media Fluid | Viscosity (at 20 °C) | Density (at 20 °C)     |
|-------------|----------------------|------------------------|
| glycerol    | 1412 Pa·s            | 1261 kg/m <sup>3</sup> |
| sebacate    | 9 mPa·s              | 912 kg/m <sup>3</sup>  |

The correct determination of these parameters is very important in terms of ease of measurement. Another factor that can affect the measurement results is the sampling frequency used when collecting data in the laser interferometer. In this respect, four sampling frequency values were determined as 10 kHz, 25 kHz, 50 kHz and 100 kHz. The factors and levels to be used in the Taguchi method are given in Table 4.

Table 4. Factors and levels for Taguchi method.

| Factors   | Level 1  | Level 2  | Level 3 | Level 4 |
|-----------|----------|----------|---------|---------|
| Piston    | p1       | p2       | p3      | p4      |
| Cylinder  | s1       | s2       | s3      | s4      |
| Frequency | 10 kHz   | 25 kHz   | 50 kHz  | 100 kHz |
| Media     | glycerol | sebacate |         |         |

If the parameter study is to be carried out according to Table 4, it is necessary to perform a total of 128 experiments. In such a case, the Taguchi method will be more efficient and easier to apply. Normally, orthogonal arrays suitable for the problem are determined by their degrees of freedom. However, special mixed-level designs are used here, since there is no equal number of levels. Among these arrays, the most suitable for us is the L16 orthogonal array, where the 3 factors have 4 levels and the 4th factor has 2 levels. The Taguchi experimental design created in this way is given in Table 5.

As can be seen in Table 5, with the Taguchi method, it is possible to determine the parameters related to only 16 experiments instead of 128 experiments. In this way, a total of 80 measurements were taken by making 5 repetitions for 16 different experiments specified in the Taguchi experimental design. After the pressure values obtained from the experiments were calculated with (3), these values were written in the Minitab program and the analysis was carried out. The response values obtained from the experiments to be used in the Taguchi experimental design are given in Table 6.

The terms M1, M2, M3, M4, and M5 in Table 6 represent the measurement series in the Taguchi experimental design. Table 6 contains some empty cells because it was noticed that acceleration data for these measurements could not be obtained after the measurements were completed.

Taguchi used the *signal-to-noise* (S/N) ratio as the preferred quality attribute. The reason for this is that as the mean decreases, the standard deviation decreases and vice versa. Therefore, instead of the standard deviation, the signal-to-noise ratio is used as a measurable value [17].

The signal-to-noise ratio is a robustness measure that can be used to determine control factor settings that minimize the effect of noise on response. The signal factor refers to the actual value received from the system, and noise factor refers to the factors that cannot be included in the experimental design but affect the test result. Noise sources are all variables that cause the desired performance characteristics to deviate from the target value. Therefore, the smaller the N value, which expresses the noise factors in the S/N ratio, the closer to the desired target value. In other words, the aim of this analysis is to maximize the S/N ratio. The Minitab program calculates a separate signal-to-noise (S/N) ratio for each combination of control factor levels in the Taguchi experimental design.

Table 5. Taguchi experimental design.

| No | Piston | Cylinder | Frequency (kHz) | Media    |
|----|--------|----------|-----------------|----------|
| 1  | p1     | s1       | 10              | glycerol |
| 2  | p1     | s2       | 25              | glycerol |
| 3  | p1     | s3       | 50              | sebacate |
| 4  | p1     | s4       | 100             | sebacate |
| 5  | p2     | s1       | 25              | sebacate |
| 6  | p2     | s2       | 10              | sebacate |
| 7  | p2     | s3       | 100             | glycerol |
| 8  | p2     | s4       | 50              | glycerol |
| 9  | p3     | s1       | 50              | glycerol |
| 10 | p3     | s2       | 100             | glycerol |
| 11 | p3     | s3       | 10              | sebacate |
| 12 | p3     | s4       | 25              | sebacate |
| 13 | p4     | s1       | 100             | sebacate |
| 14 | p4     | s2       | 50              | sebacate |
| 15 | p4     | s3       | 25              | glycerol |
| 16 | p4     | s4       | 10              | glycerol |

Table 6. Response values of the experiments.

| No | M1    | M2    | M3    | M4    | M5    |
|----|-------|-------|-------|-------|-------|
|    | MPa   | MPa   | MPa   | MPa   | MPa   |
| 1  | 52.08 | 51.80 | 52.06 | 52.69 | 52.69 |
| 2  | 51.98 | 51.40 | 51.17 | 51.23 | 51.37 |
| 3  | 38.37 | 37.69 | 37.76 | 38.00 | 37.99 |
| 4  | 38.02 | 38.40 | 39.07 | 39.81 | 40.66 |
| 5  | 39.46 | 40.74 | 41.98 |       |       |
| 6  | 36.90 | 37.01 | 37.14 | 37.46 | 37.65 |
| 7  | 52.13 | 51.85 | 51.83 | 52.04 | 52.27 |
| 8  | 53.30 | 52.17 | 53.23 | 53.60 | 54.03 |
| 9  | 52.66 | 52.40 | 52.66 | 53.27 | 53.75 |
| 10 | 53.68 | 52.53 | 52.11 | 51.80 | 52.24 |
| 11 | 37.44 | 36.85 |       | 36.87 | 36.79 |
| 12 | 38.85 | 40.22 | 41.10 | 41.77 | 42.78 |
| 13 | 41.05 | 41.57 | 44.16 |       |       |
| 14 | 37.44 | 37.66 | 37.92 | 38.18 |       |
| 15 | 52.51 | 51.38 | 51.55 | 51.46 | 51.72 |
| 16 | 50.87 | 50.89 | 51.58 | 52.62 | 53.22 |

Depending on the purpose of the study to be carried out, it is necessary to choose between different S/N ratios. For static designs, the Minitab program provides different S/N ratios: smaller is better, larger is better, and nominal is the best ratio [18]. Among these S/N ratios, the most suitable one for this study is given with (11), the nominal is the best situation.

$$\frac{S}{N} = 10 \log \left( \frac{\bar{Y}^2}{s^2} \right), \quad (11)$$

where S is the signal, N is the noise,  $\bar{Y}$  is mean of responses for the given factor level combination and  $s^2$  is the variance of the responses for the given factor level combination. The averages of the S/N values calculated for each level by the Minitab program using the experimental design in Table 5 and the response values in Table 6 are given in Table 7.

Table 7. Average of the S/N values of the parameters.

| Level | Piston | Cylinder | Frequency | Media |
|-------|--------|----------|-----------|-------|
| 1     | 40.17  | 35.03    | 39.82     | 40.59 |
| 2     | 39.59  | 41.04    | 36.01     | 35.75 |
| 3     | 36.83  | 43.70    | 40.48     |       |
| 4     | 36.09  | 32.92    | 36.37     |       |

Taguchi suggests analysing the means and the signal-to-noise ratio using a conceptual approach that involves plotting effects without using ANOVA and visually identifying factors that seem important, thus simplifying the analysis [19]. Optimal levels of the parameters always occur at the levels where the signal-to-noise ratio is the biggest. As seen in Fig. 14, the first level of piston parameter, p1, the third level of the cylinder parameter, s3, the third level of the sampling frequency parameter, 50 kHz and the first level of the media parameter, glycerol, are the optimum design parameters for this experimental design.

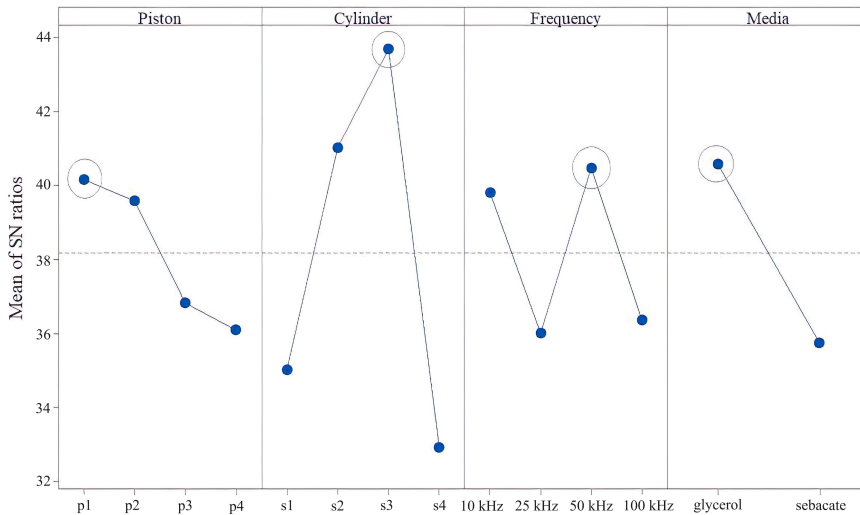


Fig. 14. Optimum parameters of the Taguchi experiment design.

## 6. Conclusions

In this study, some of the dynamic pressure measurement system parameters, which were primarily designed using the Taguchi experimental design and analysis, were determined as the optimum. It was very important for the accuracy of the study that the acceleration data, which is the most effective parameter for the reference pressure value calculations, to be used as response values in the analysis, can be obtained with high precision. Therefore, a low-pass filter selection study was carried out that minimizes the amount of high noise in the acceleration signal and it was evaluated that this value could be 1500 Hz for our study. In this way, the data obtained by examining about 80 acceleration signals were used in dynamic pressure calculations.

On the other hand, dimensional measurements were made for different designed and manufactured pistons and cylinders, and effective area calculations were made with these values. There are 16 different piston-cylinder combinations in the Taguchi experimental design, so 16 different effective area calculations were made with Dadson's theory.

We used the Taguchi method, which is the most appropriate method, to select the piston, cylinder and fluid to be used with the measuring head, and also to determine the laser interferometer sampling frequency value, which may affect the accuracy of the acceleration value. In this way, instead of 128 different experimental designs, only 16 experimental designs had to be developed and the results could be examined. Considering that we performed five repetitive measurements in each design to increase the accuracy of the measurements, we were able to complete the study with a total of 80 measurements instead of 640 measurements. As a result of the study, the first level of piston parameter (p1), the third level of the cylinder parameter (s3), the third level of the sampling frequency parameter (50 kHz) and the first level of the media parameter (glycerol) were found to be the most effective parameters to ensure repeatability in measurements and to obtain accurate acceleration data.

## References

- [1] Bilgiç, E., & Durgut, Y. (2015). Effects of waveform model on sensitivity values of transducers used in mechanical dynamic measurements. *Acta Physica Polonica A*, 128(2B), B-271. <https://doi.org/10.12693/aphyspola.128.b-267>
- [2] Durgut, Y., Bağcı, E., Akşahin, E., & İnce, A. T. (2017). An investigation on characterization of dynamic pressure transducers using material impact test machine. *Journal of the Brazilian Society of Mechanical Sciences and Engineering*, 39(9), 3645–3655. <https://doi.org/10.1007/s40430-017-0763-3>
- [3] Bean, V. E. (1994). Dynamic Pressure Metrology. *Metrologia*, 30(6), 737–741. <https://doi.org/10.1088/0026-1394/30/6/037>
- [4] Hjelmgren, J. (2002). *Dynamic Measurement of Pressure – A Literature Survey*. SP Measurement Technology Report, SP Swedish National Testing and Research Institute.
- [5] Bartoli, C., Beug, M. F., Bruns, T., Elster, C., Esward, T. J., Klaus, L., Knott, A., Kobusch, M., Saxholm, S., & Schlegel, C. (2012). Traceable dynamic measurement of mechanical quantities: objectives and first results of this European project. *International Journal of Metrology and Quality Engineering*, 3(3), 127–135. <https://doi.org/10.1051/ijmqe/2012020>
- [6] Choi, I., Yang, I., & Woo, S. (2013). High dynamic pressure standard based on the density change of the step pressure generator. *Metrologia*, 50(6), 631–636. <https://doi.org/10.1088/0026-1394/50/6/631>
- [7] Lally, J. F. (1991, April). Dynamic step-pressure calibration. In *Proceedings from the NIST workshop on the measurement of transient pressure and temperature*, Gaithersburg, Maryland, USA (pp. 104-119).



- [8] Salminen, J., Högström, R., Saxholm, S., Lakka, A., Riski, K., & Heinonen, M. (2018). Development of a primary standard for dynamic pressure based on drop weight method covering a range of 10 MPa–400 MPa. *Metrologia*, *55*(2), S52–S59. <https://doi.org/10.1088/1681-7575/aaa847>
- [9] Slanina, O., Quabis, S., Derksen, S., Herbst, J., & Wynands, R. (2020). Comparing the adiabatic and isothermal pressure dependence of the index of refraction in a drop-weight apparatus. *Appl. Phys. B* *126*, 175, <https://doi.org/10.1007/s00340-020-07519-z>
- [10] Salminen, J., Saxholm, S., Hämäläinen, J., & Högström, R. (2020). Advances in traceable calibration of cylinder pressure transducers. *Metrologia*, *57*(4), 045006. <https://doi.org/10.1088/1681-7575/ab8fb9>
- [11] Karna, S. K., & Sahai, R. (2012). An overview on Taguchi method. *International Journal of Engineering and Mathematical Sciences*, *1*(1), 11-18.
- [12] Taguchi, G. (1993). Robust technology development. *Mechanical Engineering-CIME*, *115*(3), 60-63.
- [13] Molinar, G. F., Rebaglia, B. I., Sacconi, A., Legras, J. C., Vailliau, G., Schmidt, J. W., Stoup, J. R., Flack, D. R., Sabuga, W., & Jusko, O. (1999). CCM key comparison in the pressure range 0.05 MPa to 1 MPa (gas medium, gauge mode). Phase A1: Dimensional measurements and calculation of effective area. *Metrologia*, *36*(6), 657–662. <https://doi.org/10.1088/0026-1394/36/6/34>
- [14] Molinar, G. F., Bergoglio, M., Sabuga, W., Otal, P., Ayyildiz, G., Verbeek, J., & Farár, P. (2005). Calculation of effective area  $A_0$  for six piston–cylinder assemblies of pressure balances. Results of the EUROMET Project 740. *Metrologia*, *42*(6), S197–S201. <https://doi.org/10.1088/0026-1394/42/6/s11>
- [15] Dadson, R. S., Lewis, S. L., & Peggs, G. N. (1982). *The Pressure Balance: Theory and Practice*. Her Majesty's Stationery Office.
- [16] Elkarous, L., Robbe, C., Pirlot, M., & Golinval, J. (2016). Dynamic calibration of piezoelectric transducers for ballistic high-pressure measurement. *International Journal of Metrology and Quality Engineering*, *7*(2), 201. <https://doi.org/10.1051/ijmqe/2016004>
- [17] Ghani, J. A., Choudhury, I. A., & Hassan, H. (2004). Application of Taguchi method in the optimization of end milling parameters. *Journal of Materials Processing Technology*, *145*(1), 84–92. [https://doi.org/10.1016/s0924-0136\(03\)00865-3](https://doi.org/10.1016/s0924-0136(03)00865-3)
- [18] Minitab, LLC. *Methods and formulas for analyze Taguchi design*. Retrieved January 31, 2024. <https://support.minitab.com/en-us/minitab/20/help-and-how-to/statistical-modeling/dae/how-to/taguchi/analyze-taguchi-design/methods-and-formulas/methods-and-formulas/>
- [19] Phadke, M. S. (1995). *Quality Engineering Using Robust Design*. Prentice Hall PTR.

**Recep Yılmaz** received his M.Sc. degree in mechanics from the Mechanical Engineering Department of Necmettin Erbakan University, Turkey in 2019. He has continued his Ph.D. program in mechanical engineering at Necmettin Erbakan University then. He is currently employed as a senior researcher in the pressure laboratory of the Turkish National Metrology Institute. Dynamic pressure, static pressure, mechanical design, finite element analysis and measurement systems are among his interest areas.

**Yasin Durgut** works as a chief expert researcher in charge of the pressure laboratory at the Turkish National Metrology Institute. He holds a Ph.D. degree in Physics. His areas of expertise include static and dynamic pressure measurements. He has provided training and consultancy to more than 100 companies. He carries out accreditation assessments within the ISO EN/IEC 17025 standards. He has taken part in about 10 different research projects in the field of pressure. He is a member of the BIPM Mass and Related Quantities Consultative Committee and the EURAMET Mass and Related Quantities Committee pressure working group. He has over 50 publications in the field of pressure metrology in journals and conferences.

**Hüseyin Arıkan** received his B.Sc. (1989), M.Sc. (1993) and PhD (2002) degrees in mechanics from the Department of Mechanical Engineering of Selçuk University, Turkey. He is a Professor in Mechanical Engineering of Necmettin Erbakan University, Turkey. His main areas of interest are Composite Materials, Fracture Mechanics and Materials Design and Manufacturing.

**Abdullah Hamarat** graduated from the Department of Mechanical Engineering of Istanbul Technical University (ITU) in 1996 and completed his master's degree at the ITU Institute of Science and Technology, Department of Energy in 2002. He works as a researcher in the pressure laboratory at the Turkish National Metrology Institute. He is experienced in the field of static pressure calibrations and provides training and consultancy services in the field of static pressure calibrations. He carries out accreditation assessments within the ISO EN/IEC 17025 standards. He is a member of the auditor pool of the Turkish Accreditation Agency and takes part in audit duties on behalf of this institution.